Building and Environment 110 (2016) 115–128

Contents lists available at ScienceDirect

Building and Environment

journal homepage: www.elsevier.com/locate/buildenv

Developing an empirical model for roof solar chimney based on experimental data from various test rigs

Long Shi [a, *], Guomin Zhang [a], Xudong Cheng [b], Yan Guo [c], Jinhui Wang [d], Michael Yit Lin Chew [e]

[a] Civil and Infrastructure Engineering Discipline, School of Engineering, RMIT University, GPO Box 2476, Melbourne, VIC, 3001, Australia
[b] State Key Laboratory of Fire Science, University of Science and Technology of China, Hefei, Anhui, 230026, PR China
[c] Department of Urban Planning, School of Urban Design, Wuhan University, 430072, PR China
[d] College of Ocean Science and Engineering, Shanghai Maritime University, Shanghai, 201306, PR China
[e] Department of Building, National University of Singapore, Singapore, 117566, Singapore

ARTICLE INFO

Article history:
Received 15 July 2016
Received in revised form
7 October 2016
Accepted 7 October 2016
Available online 8 October 2016

Keywords:
Roof solar chimney
Inclination angle
Cavity gap
Solar radiation
Height air gap ratio
Empirical model

ABSTRACT

Roof solar chimney is one type of solar chimney to enhance the natural ventilation in buildings. Under the factor that previous studies numerically modelled and validated their results by single test rig, experimental data from all the possible test rigs in the literature were collected and analysed in this study to develop an empirical model for general use. This empirical model was validated by experimental data from various test rigs, with an average error of 14% and up to 144.6% error. Based on the experimental data from different test rigs, the influences of several factors, such as calculated inclination angle (θ', shown in Eq. (6)), cavity gap (d), width (w), height (H), height/cavity gap ratio (H/d), inlet area (A_{in}), outlet area (A_{out}) and radiation heat (q), on solar chimney performance were addressed. The volumetric flow rate of roof solar chimney showed a linear relationship with $w(\sin\theta')^{1/3}q^{1/2}d^{0.7}H^{2/3}$. The slope of this linear relationship can be determined by test environment, cavity material, glazing, and insulation conditions. Those experimental data within a H/d range of 2.5–103.5 showed that the air velocity increases with a larger H/d, but the volumetric flow rate behaves in an opposite way. It is known from experiments that an equal inlet and outlet area can enhance the flow rate in the cavity and for unequal openings the outlet area showed a relatively higher importance in promoting the air flow.

1. Introduction

Under increasingly severe environment pollution and energy crisis caused by continued exploitation and overuse of fossil energy, applications of renewable energy have become a critical topic [1–3]. Buildings consume nearly 40% of total energy use in United States and about 50% of the energy is used for heating, ventilating and cooling the space [4]. Natural ventilation is an important sustainable building design strategy which is known to mankind for centuries, and has attracted a strong growing interest because of its potential advantages over mechanical ventilation systems in terms of energy requirement, economic and environmental benefits [5]. Solar chimney as one of the reliable systems to enhance natural ventilation has attracted increasing attentions from engineers because of their long life energy saving for buildings.

Solar chimney is basically a solar air heater, which is vertically or horizontally embedded as a part of wall or roof. The classification of solar chimney can be varied according to different configurations or functions [6]. Roof solar chimney is one type of solar chimney mounted on the roof top in which the absorber is inclined at some angle to capture maximum solar radiation. It is used to enhance buoyance driven natural ventilation, which is similar to wall solar chimney or Trombe wall [7]. A solar chimney house can reduce the average daily electrical consumption of an air-conditioner by 10–20% [8] and decrease the fan shaft requirement by about 50% and even 90% in some specific months [9]. It can bring in long life energy saving with an only 0–15% extra design and construction cost.

* Corresponding author.
E-mail addresses: shilong@mail.ustc.edu.cn, long.shi@rmit.edu.au (L. Shi).

http://dx.doi.org/10.1016/j.buildenv.2016.10.002
0360-1323/

Nomenclature

a	coefficient during correlation
A	area (m^2)
b	coefficient during correlation
C	coefficient
C_p	specific heat capacity (J/kg °C)
d	air gap thickness (m)
D_h	hydraulic diameter of cavity (m)
E	test environment, shown in Eq. (18)
f	wall friction coefficient
g	gravitational acceleration (m/s^2)
G	glazing, shown in Eq. (18)
h	heat transfer coefficient (W/m °C)
H	cavity height (m)
I	insulation, shown in Eq. (18)
k	pressure loss coefficient
m	mass flow rate (kg/s)
M	cavity material, shown in Eq. (18)
N	number of collected experiments tests
q	heat input intensity (W/m^2)
Q	heat input (W)
Slope	regressed slope, obtained by Eq. (18)
T	temperature (°C)
u	velocity in the cavity (m/s)
V	volumetric flow rate (m^3/s)
$\overline{V}$	volumetric flow rate per meter wide ($m^3/s \cdot m$)
w	cavity width (m)

Greek letters

α	thermal expansion coefficient (1/°C)
θ	inclination angle from the horizontal (°)
θ'	calculated inclination angle in Eq. (6)
ρ	density (kg/m^3)

Subscripts and superscripts

c	cavity
d	discharge
i	experiment number
in	inlet
out	outlet
r	ratio between outlet and inlet
0	ambient conditions

Most of the previous parametric studies were based on numerical approaches and previous experimental tests have been focused on limited number of influencing factors. The lacking of experimental tests on various influencing factors is because of the complicated configurations and also high costs for experimental tests [10,11]. This is the reason why 70% of the related studies are based on numerical models [12]. Although these numerical models are able to provide detailed information to engineers, the construction of the model is complicated that it also needs a long calculation time [9,13,14]. Therefore, comparing to the numerical models, theoretical and empirical models are more convenient to the engineering designs.

Although many theoretical and empirical models have been developed to predict the performance of solar chimney, these models have been developed based on one experimental rig, mostly preventing their applications and predictions on various-sized solar chimney. This is because single experimental rig is usually limited in conducting parametric study, usually one or two parameters. The empirical model developed based on configuration of single test rig may not be appropriately applicable to other configurations. Even some models may be applicable to several experimental rigs, but their applicability to various test rigs are not known yet. Another shortcoming of previous models is the difficult-to-get inputs, such as wall friction coefficient [15], pressure loss coefficient [16], thermal expansion coefficient [17] and geometrical configuration factor [18].

Therefore, in this study, an investigation has been conducted based on previous experimental data from various test rigs to address all the possible influencing factors. Moreover, an empirical model was developed to predict the volumetric flow rate of roof solar chimney. The objectives of this study are:

- To determine the key influencing factors on the performance of roof solar chimney;
- To develop an empirical model to predict the airflow rate of roof solar chimney under various conditions; and
- To provide a technical guide for the optimization design of roof solar chimney.

2. Methodology

2.1. Suitability of the experimental tests

Fig. 1 shows a schematic of a typical test rig for roof solar chimney. The test rig can be tilted with different inclination angles (θ from horizontal), usually from 0° to 90°. The dimension of the roof solar chimney is w (width) × H (height) × d (air gap thickness). The surface and bottom sides are parallel. The exposed surface is usually built by glass, allowing the penetration of radiation through the transparent glass. The other three sides are usually constructed by non-transparent materials, such as wood or concrete. The bottom side, opposite to the glass, is covered by insulating materials, which can benefit the heating up processes of the air in the cavity and reducing heat losses to the outside environment. Under high temperature, the air in the cavity rises up under the buoyancy,

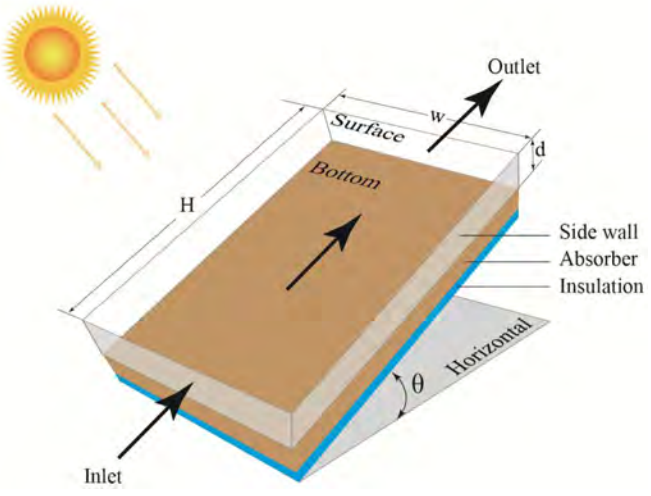

Fig. 1. Schematic of a typical test rig for roof solar chimney.

Table 1
A summary of experimental tests collected from the literature.

Author	Year	Location	Size	Cavity materials
Imran et al. [20]	2015	Baghdad, Iraq	2.0 m (H) × 2.0 m (w) × 0.05–0.15 m (d)	Aluminium sheet and a glass panel
Saifi et al. [21]	2012	Quargla, Algeria	2.0 m (H) × 1.0 m (w) × 0.1–0.3 m (d)	Iron sheet and a glass panel
Somsila et al. [22]	2010	Thailand[b]	1.0–2.0 m (H) × 0.5 m (w) × 0.1 m (d)	Wood structure and glass
Ryan [23]	2008	Glasgow, UK	0.521–2.07 m (H) × 0.925 m (w) × 0.02–0.15 m (d)	Plasterboard and transparent Perspex
Susanti et al. [19] [a]	2008	Toyohashi, Japan[b]	4.882 m (H) × 0.4 m (w) × 0.078 m (d)	Plywood
Burek and Habeb [24]	2007	Glasgow, UK	1.205 m (H) × 0.925 m (w) × 0.02–0.11 m (d)	Plasterboard and transparent Perspex
Mathur et al. [25]	2006	Jaipur, India	1.0 m (H) × 1.0 m (w) × 0.35 m (d)	Aluminium sheet and a glass
Ryan et al. [26]	2005	Glasgow, UK	0.5 m (H) × 1.0 m (w) × 0.02–0.15 m (d)	Plasterboard and transparent Perspex
Zhai et al. [27] [a]	2005	Shanghai, China	1.5 m (H) × 0.5 m (w) × 0.1–0.5 m (d)	Wood plank
Chen et al. [28]	2003	Victoria, Australia[b]	1.5 m (H) × 0.62 m (w) × 0.1–0.6 m (d)	Bottom side of stainless-steel shim with other three sides of Plexiglas
Khedari et al. [29] [a]	2002	Thailand	1.36 m (H) × 0.68 m (w) × 0.14 m (d)	Plywood
Adam et al. [30]	2002	Osaka, Japan	2.0 m (H) × 1.0 m (w) × 0.1–0.3 m (d)	Aluminium wall and a glass panel

Note.
[a] The experimental rigs do not contain a front glass and a self-heating wall was used, replacing by a non-transparent slab; and.
[b] There is no specific description of experimental location in the context, so the locations of the first author were used.

resulting in natural ventilation of the inside environment.

To address the effects of designing factors, such as width, height and inclination angle, on the performance of roof solar chimney, experimental data in the literature have been collected. All the literature are primary source. For all the analysed test rigs, the surface and bottom are parallel panels, resulting in an equal area of inlet and outlet, excepting the test rig built by Susanti [19] that it was used to address the influences of inlet and out areas on the performance. In Susanti's experiment, the surface and bottom of the cavity were constructed by parallel panels, but the inlet and outlet were not fully opened, which were covered by aluminium plate to construct models with different inlet and outlet ratios.

To explore the influences of factors on the performance, those experimental tests we have selected are able to clearly show the test conditions, such as measurement methods, test environment, cavity materials, glazing, and heating and insulation methods. Once the literature was selected, all the experimental data in the literature were used for the analysis. Solar chimneys coupling with other renewable energy techniques, such as ground source heat pump and photovoltaic module, were not considered in this study as it is difficult to address the influence of single parameter on its performance. After that, surprisingly, there are very limited experimental tests available in the literature, as shown in Table 1.

It should be noticed from Table 1 that there are two kinds of experimental rigs, namely with and without transparent exposed surface. Practically, a transparent surface is needed in order to heat up the air in the cavity by passing through solar radiation. Transparent glass, and Perspex and Plexiglas are usually utilized for the surface, excepting that three sides (two sidewalls and surface) are transparent plexiglass in Chen et al.'s test [28]. The frames of most of the cavities were made of timber or aluminium sheet.

Several testing conditions exist in the previous experiments. For example, Imran et al. [20] installed the roof solar chimney to a 2 m (width) × 3 m (length) × 2 m (height) room, collecting the data for daytime from 7:00 am to 2:00 pm during various day. Mathur et al. [25] connected the roof solar chimney with a cubical wooden chamber of 1 m × 1 m × 1 m. Saifi et al. [21] measured the data with single roof solar chimney without connecting with a room, and the date were measured from 9:00 am to 4:00 pm. Besides the tests carried out in open space, Somsila et al. [22] conducted the experiment in indoor environment and used the equipment to produce light intensity instead of obtaining the sunlight. In some experiments [19,24,27,29], to simulate the solar radiation, the bottom side of the cavity was heated up using electric heating plate.

Some tests were performed outside with possible wind effect. Imran et al. [20] mentioned that the wind effect was neglected because of small value. To reduce the effect of wind velocity, Mathur et al. [25] placed a wall having double height and triple width compared to the model on the suction side. Chen et al. [28] conducted the test in a 5 m × 7 m × 3.9 m bay to reduce the

Table 2
A summary of influencing factors and their testing ranges in literature.

Influencing factor	Unit	Studied range	Test range[a]
Inclination angle (θ)	°	10–90	15-60 [20]; 30–45 [21]; 10–90 [27]; 30–90 [28]; 30–90 [30];
Cavity gap (d)	m	0.02–0.6	0.05–0.15 [20]; 0.1–0.3 [21]; 0.02–0.15 [23]; 0.02–0.11 [24]; 0.02–0.15 [26]; 0.1–0.5 [27]; 0.1–0.6 [28]; 0.1–0.3 [30];
Height (H)	m	0.521–2.07	1.0–2.0 [22]; 0.521–2.07 [23];
Height/gap ratio (H/d)	–	2.5–103.5	13.3–40.0 [20]; 6.7–20.0 [21]; 10.0–20.0 [22]; 3.5–103.5 [23]; 9.3–51.3 [24]; 3.3–25.0 [26]; 3.0–5.0 [27]; 2.5–15.0 [28]; 6.7–20.0 [30];
Inlet area (A_{in})	m^2	0.019–0.372	0.1–0.3 [20]; 0.1–0.3 [21]; 0.02–0.15 [23]; 0.019–0.102 [24]; 0.02–0.15 [26]; 0.05–0.25 [27]; 0.062–0.372 [28]; 0.1–0.3 [30];
Outlet area (A_{out})	m^2	0.02–0.372	0.1–0.3 [20]; 0.1–0.3 [21]; 0.02–0.15 [23]; 0.02–0.15 [26]; 0.05–0.25 [27]; 0.062–0.372 [28]; 0.1–0.3 [30];
Inlet/outlet ratio (A_r)	–	0.128–7.8	0.128–7.8 [19]
Radiation heat (q)	W/m^2	50–1057	150-750 [20]; 400–800 [22]; 188–1057 [23]; 50–150 [19]; 200–1000 [24]; 500–750 [25]; 200–925 [26]; 120–650 [27]; 200–400 [28]; 73–374 [29]; 100–500 [30];

Note.
[a] This table only includes the data with parametric studies, ignoring fixed configurations.

effects of outside environment.

2.2. Data selections

Only the data from experimental tests were selected in this study, excluding numerical results. Those tests should mention cavity size (H, d, w), radiation heat (q), inclination angle (θ), average velocity (u) and volumetric flow rate (V). All the data were unified for a better comparison in the aspect of unit and configuration. For example, in an experiment done by Chen et al. [28], the inclination angle was considered between vertical panel and chimney cavity. For unification, these angles were converted to the ones between chimney cavity and the horizontal, shown in Fig. 1. It should be noticed that all the air velocity are the average velocity in the cavity, not at the inlet or outlet.

Some experimental data were obtained by a long time period

Table 3
A summary of mathematical models for roof solar chimney.

Reference	Year	Schematic	Mathematical model
Ryan and Burek [32]	2010		$m \propto q^{0.459}$; $m \propto d^{0.756}$; $m \propto H^{0.600}$
Sakonidou et al. [15]	2008	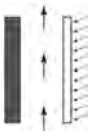	$V = sin\theta A_{out}\sqrt{\frac{2gH(\rho_0-\rho_c)}{\left(f\frac{H}{D_h}+k_{in}+k_{out}\right)\rho_c}}$
Sakonidou et al. [15]	2008		$V = C_d sin\theta \frac{\rho_c}{\rho_0} A_o \sqrt{\frac{gH(T_c-T_0)}{T_0}}$
Burek and Habeb [24]	2007		$m \propto Q^{0.572}$; $m \propto d^{0.712}$
Ryan et al. [26]	2005		$m \propto q^{0.452}$; $m \propto d^{0.652}$; $m \propto H^{0.539}$
Halldorsson et al. [16]	2002	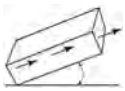	$V = A\left\{\frac{gqwsin\theta H^2}{A\rho C_p T_0\left[f\frac{H}{D_h}+k_{in}\left(\frac{A}{A_{in}}\right)^2+k_{out}\left(\frac{A}{A_{out}}\right)^2\right]}\right\}^{1/3}$
Afonso and Oliveira [17]	2000	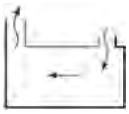	$V = A_{out}\sqrt{\frac{2\alpha g(T_c-T_0)H}{f\frac{H}{D_h}+k_{in}\left(\frac{A_{out}}{A_{in}}\right)^2+k_{out}}}$
Sandberg and Moshfegh [18]	1998		$V = A\left[\frac{gqH^2 sin\theta}{\rho_0 C_p T_0 d\left(2f\frac{H}{d}+k_{in}+1\right)}\right]^{1/3}$
Bansal et al. [33]	1993		$V = C_d A_{out}\sqrt{\frac{2(T_c-T_0)gHsin\theta}{T_0(1+A_r^2)}}$
Awbi and Gan [34]	1992		$V = C_d A\sqrt{\frac{4gH(T_c-T_0)}{T_c}}$

tests (e.g. a whole day) under solar radiation. Those data were included by averaging the data from each configuration if it is sure from the experimental description that the other influencing factors kept the same excepting the analysed factor. Excepting that, all others data were obtained when the air velocity were at steady state. In some tests [19], the model was allowed to run at least 20 h until a thermally steady condition was achieved. Table 2 shows a summary of the influencing factors and their testing ranges in the literature. The vertical test rigs were considered as an inclination angle of 90°.

In all the experimental data collected in this study, the devices showed good measuring accuracy. Imran et al. [20] used a hot wire anemometer (PCE-423 model) with a resolution of 0.01 m/s and accuracy of ±0.05–0.1 m/s. The solar radiation was measured by a solar power meter having least-count of 0.1 W/m^2 and accuracy of ±1%. The hot wire anemometer used by Somsila et al. [22] has an even better accuracy of ±0.01 m/s. Zhai et al. [27] used a hot bulb anemometer (Type ET3-2A) for which the certainty of measurement is ±0.02 m/s within a range from 0.05 to 1.0 m/s. Chen et al. [28] used a TSI8455 air velocimeter probe with a calibrated accuracy of ±5% at 0.05 m/s and a Drager smoke tube was used to identify the velocity direction. Khedari et al. [29] utilized a wattmeter (Elima model 8071) to record the power supplied to the heater.

2.3. Acquirement and analysis of the data

Some previous experimental data are presented in the form of figures. Under this situation, the best solution is to approach the authors to get the exact data. If it is impossible, a free software package developed by Thunderhead, namely DigXY, was used to obtain the data from those figures. The obtained data were tested with known data. For example, for heat flux within 150–750 W/m^2, the error of the data obtained during the test can be controlled within 0.82%, which is less than the measurement error mentioned above.

To make a better comparison, only air velocity in the solar chimney cavity were analysed. For those cases that the inlet and outlet areas are different from the cavity cross-section area, the air velocities at the inlet and outlet were converted to the air velocities for the cross-section of the cavity. Other parameters, such as mass flow and air change per hour (ACH), are not used for comparison as they are dependent on the room and cavity configurations. If the data in the literature are in the format other than air flow velocity or volumetric flow rate, these data were converted based on their configurations. During the conversion, an air density of 1.204 kg/m^3 was assumed [31]. It should be noticed that the volumetric flow rate have been converted to volumetric flow rate per meter width (m^3/s·m) in this study for a better comparison as various wide chimney cavities were used in the literature.

In some tests, more than one point was measured in the cavity. An average of air velocity was then used to represent the relevant air flow under various scenarios. For the tests with full-day measurement, average data through the whole day were utilized to represent one scenario. Some tests may have too many experimental combinations such as cavity gap, height and radiation heat. For example, Ryan [23] conducted the tests with five radiation fluxes, six cavity gaps and three chimney heights. If it needs to address the influence of chimney heights on the performance, 30 combinations were obtained from one test rig. To make a better comparison, another parameter such as radiation flux or cavity gap was selected for averaging. If we choose to average the radiation flux, the number of combinations can be reduced to 6.

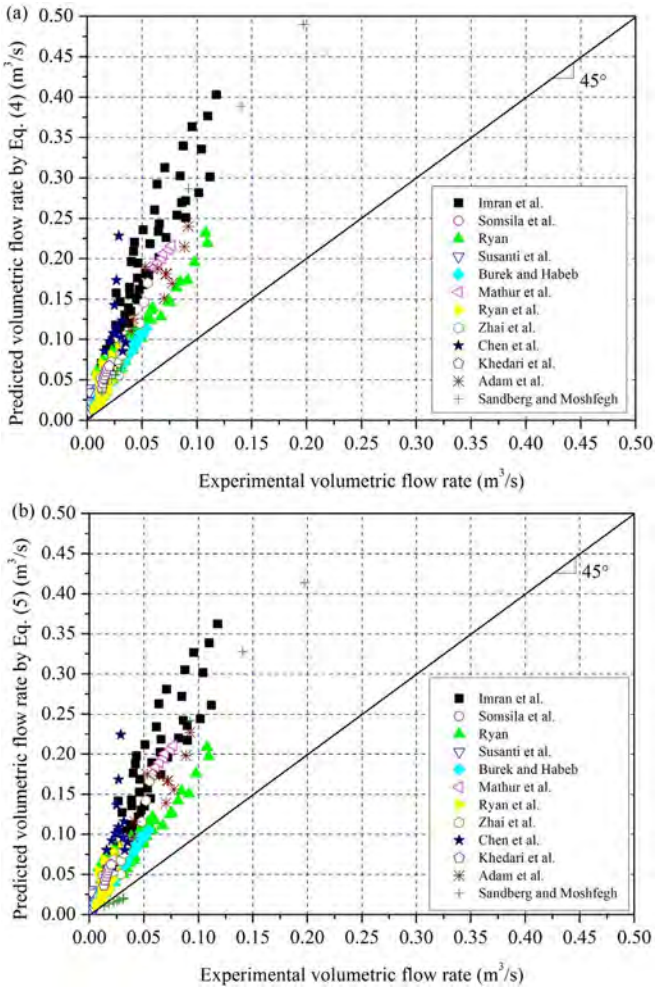

Fig. 2. A comparison between the experimental data and predictions based on: (a) Eq. (4); and (b) Eq. (5).

3. Previous mathematical models

Table 3 shows a summary of mathematical models which can be possibly applicable to roof solar chimney. These mathematical models were cited from the relevant references, which did not necessarily represent that all the models were developed by the given authors. These mathematical models were deduced or regressed based on single test rig. To show the application of these models, schematics of solar chimney revised from the original sources are included in this table.

Based on Table 3, it can be known that there are four types of mathematical models which can be applicable to roof solar chimney. The classification of the four mathematical models is dependent on the modelling inputs, such as predictions based on single parameter, air temperature, air density, and external radiation. The typical models for these four types are listed below, which did not mean that only these listed models are used in the following analysis. The function of these models is to provide a guide on the development of our empirical model, such as addressing the influence of some factors on the performance of roof solar chimney.

The first type was developed by Ryan et al. [24,26,32] by correlating experimental data with a form of,

$$m \propto q^{0.459}; m \propto d^{0.756}; m \propto H^{0.600} \quad (1)$$

where $\propto$ represents a proportional relationship between the terms at two sides. This equation indicates that the mass flow rate in the chimney cavity has a proportional relationship with $q^{0.459}$, $d^{0.756}$, and $H^{0.600}$, respectively.

The second type models are based on the air temperature in the cavity with the need of a discharge coefficient. This type of model is obtained by theoretical deduction compromised with some assumptions. Sometimes their applications may be limited because of the difficult-to-get inputs, such as mean air temperature in the cavity. The model developed by Bansal et al. [33] is one of them,

$$V = C_d A_{out} \sqrt{\frac{2(T_c - T_0) g H sin\theta}{T_0\left(1 + A_r^2\right)}} \quad (2)$$

The third type is based on the input of air density in the cavity. The prediction is similar to the second type, replacing the needs of air temperature with air density. The model from Sakonidou et al. [15] can be given by,

$$V = sin\theta A_{out} \sqrt{\frac{2gH(\rho_0 - \rho_c)}{\left(f\frac{H}{D_h} + k_{in} + k_{out}\right)\rho_c}} \quad (3)$$

The last type is the direct prediction based on radiation flux (or heat supply). Some of the mathematical models need a large number of inputted parameters, such as discharge coefficient, wall friction coefficient, and pressure loss coefficient. Two typical models are from Sandberg and Moshfegh [18] and Halldorsson et al. [16], respectively,

$$V = A\left[\frac{gqH^2 sin\theta}{\rho_0 C_p T_0 d\left(2f\frac{H}{d} + k_{in} + 1\right)}\right]^{1/3} \quad (4)$$

$$V = A\left\{\frac{gqwsin\theta H^2}{A\rho C_p T_0\left[f\frac{H}{D_h} + k_{in}\left(\frac{A}{A_{in}}\right)^2 + k_{out}\left(\frac{A}{A_{out}}\right)^2\right]}\right\}^{1/3} \quad (5)$$

All the experimental data found in the literature provided only radiation flux, not the air density and air temperature in the cavity. So only the fourth type of models can be compared with experimental data, namely Eqs. (4) and (5). The values for coefficients are obtained from Reference [16].

A comparison between the predictions of Eqs. (4) and (5) and experimental data can be seen in Fig. 2. It is observed that the predicted values are much larger than those experimental data. This may be because of the modelling input, such as wall friction coefficient and pressure loss coefficient [3]. These are the coefficients which are dependent on test rig. Chen et al. [28] observed a similar phenomenon and indicated the discrepancy may be because of the underestimated pressure losses.

Under the fact of the overprediction of previous mathematical models, the influences of factors on the performance of roof solar chimney will be addressed one by one based on experimental data in the following sections. Eventually, an empirical model will be developed with a better accuracy for various test rigs under different situations.

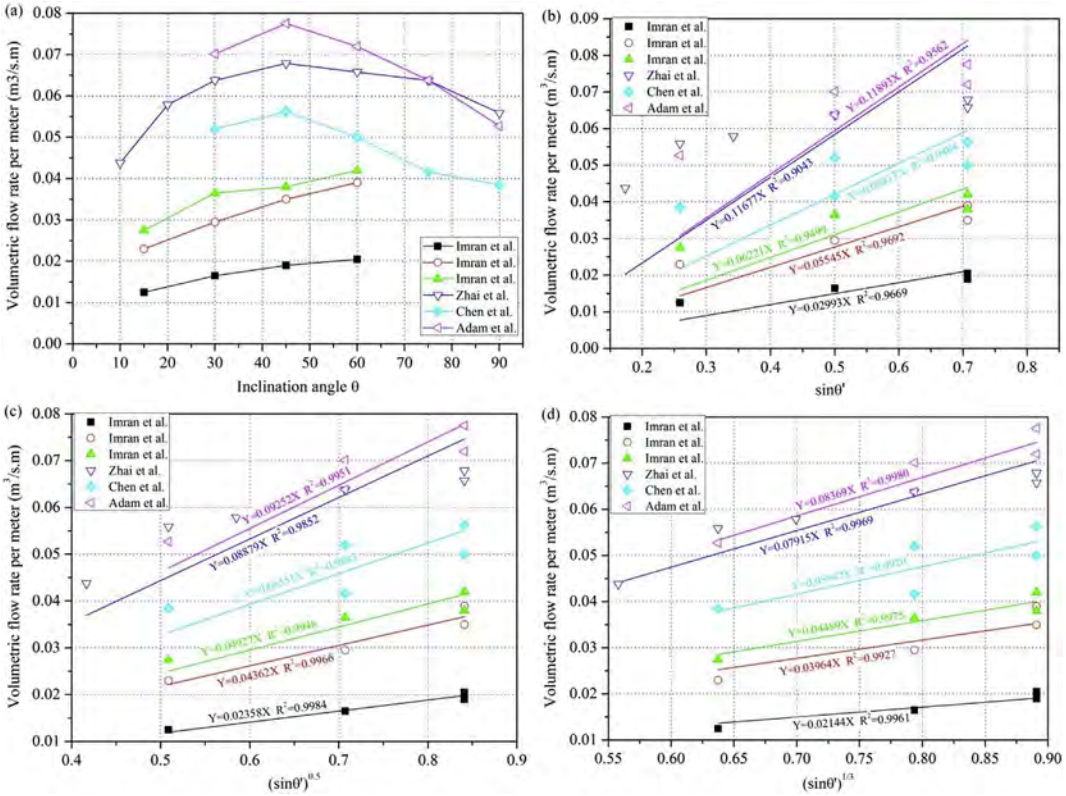

Fig. 3. Relationship between volumetric flow rate and: (a) θ; (b) $sin\theta'$; (c) $(sin\theta')^{1/2}$; and (d) $(sin\theta')^{1/3}$.

4. Results and discussion

4.1. Inclination angle

As roof solar chimney is installed on rooftop or other related place, the inclination angle is one of the important factors regarding the absorption of solar radiation. The reason for the tilted solar chimney to enhance the natural ventilation is the reduction in pressure loss [28]. As the roof solar chimney is fixed after installation, the best inclination angle is then significant to determine the performance of the solar chimney. It is known from Table 2 that the testing range of inclination angle in previous studies is 10–90°.

Fig. 3(a) shows the volumetric flow rate per meter width with various inclination angles. It can be seen that the maximum flow rate happen at an inclination angle of 45°, excepting those of 60° from Imran et al. [20]. It should be noticed that the three lines from Imran et al. [20] address the influence of inclination angle on volumetric flow rate under three cavity gaps. This is also applied to the following figures that different lines were provided for one source when those experimental data represent various influencing factors.

It can be observed from Fig. 3(a) that there are two optimum inclination angles from different experimental tests, namely 45° and 60°. These experimental data show a symmetry distribution around the optimum inclination angle. The airflow rate increase from 0° until the optimum inclination angle, and it then decreases after that. Therefore, $\sin\theta$ cannot cover the predictions within the whole range of 0–90° as $\sin\theta$ keeps increasing within this range. Especially, for vertical solar chimney, namely an inclination angle of 90°, $\sin\theta$ is equal to 0. It means the prediction based on $\sin\theta$ can only cover the inclination angle below the optimum inclination angle.

Based on Fig. 3(a), it can be seen that for vertical solar chimney (90°), its volumetric flow rate is equal to the solar chimney with an inclination angle between 10 and 20°. In addition, the exact optimum inclination angle would not coincidently be 45° or 60° as those previous experimental tests have been done with an interval of 15°. The exact optimum inclination angle could be between 45 and 60°. Considering the above conditions, an optimum inclination angle of 52.5° is assumed by averaging the two optimum inclination angles in Fig. 3(a). We then define a calculated inclination angle,

$$\theta' = \begin{cases} \theta, & \theta \le 52.5 \\ 105 - \theta, & \theta > 52.5 \end{cases} \quad (6)$$

Based on Eq. (6), it can be known that the predicted volumetric flow

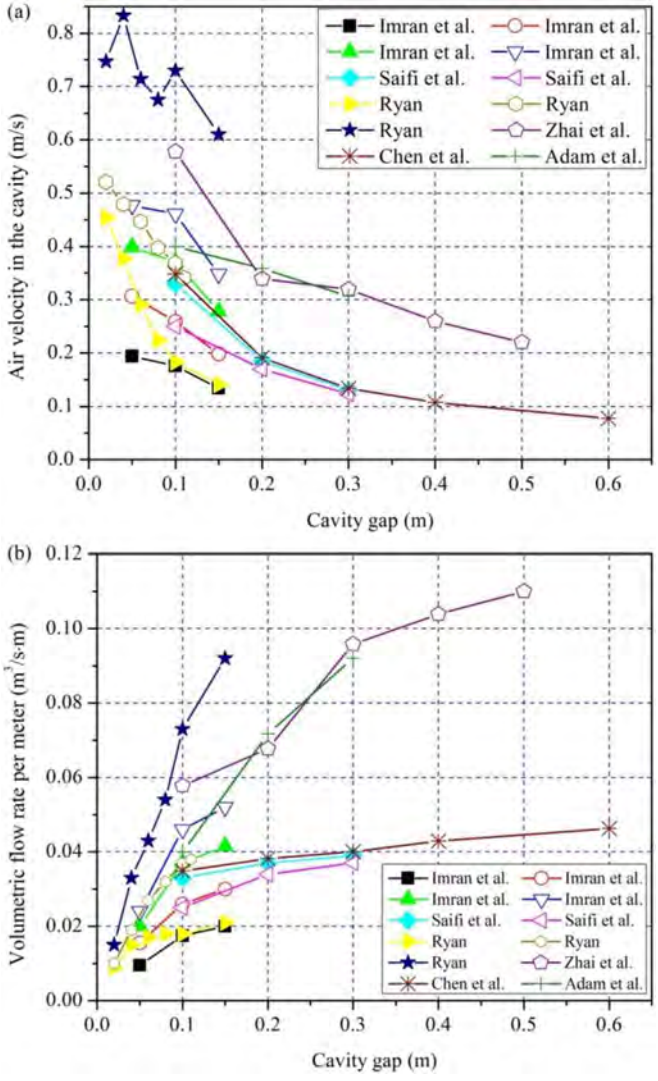

Fig. 4. The influence of cavity gap on: (a) air velocity; and (b) volumetric flow rate.

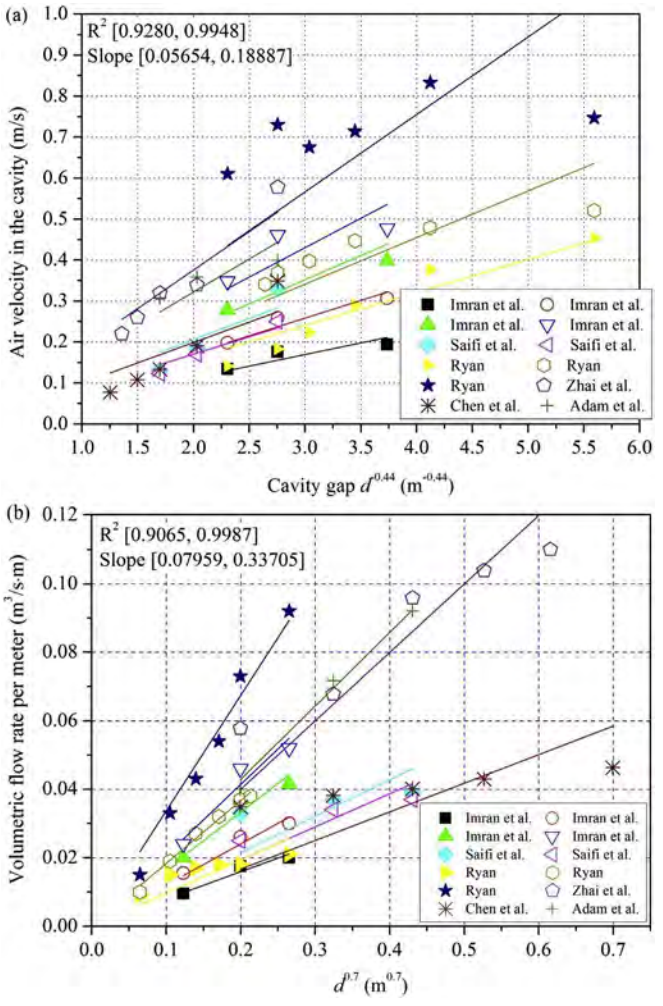

Fig. 5. Correlation between cavity depth and: (a) air velocity in the cavity; and (b) volumetric flow rate per meter.

rate of vertical solar chimney will be equal to the solar chimney with an inclination angle of 15°. It is consistent with the previous experimental tests shown in Fig. 3(a).

The volumetric flow rates are corrected with $\sin\theta'$, $(\sin\theta')^{1/2}$, and $(\sin\theta')^{1/3}$, respectively, as shown in Fig. 3(b)–(d). The experimental volumetric flow rate show the best fit with $(\sin\theta')^{1/3}$ based on the R^2 values during the regression. The relationship can be expressed by,

$$\overline{V} \propto (sin\theta')^{1/3} \tag{7}$$

It can be known that Eq. (7) is able to predict solar chimney with an inclination angle of 10–90°. This is determined by the symmetry distribution of volumetric flow rate around the optimum inclination angle.

4.2. Cavity gap

In the chimney cavity, the air with a higher temperature is driven upward by buoyancy. As the temperature rise is much dependent on the external solar radiation, a solar absorber at the bottom of the cavity is used to absorb the radiation. The heating up process of the air in the cavity is much dependent on the distance of the air to the solar absorber, namely cavity gap. Fig. 4 shows the influence of cavity gap on the performance of roof solar chimney. According to Fig. 4(a), it is observed that the air velocity in the cavity drop with a bigger cavity gap, same with Reference [35]. This can be explained by the convection heat transfer. For a thin cavity, the heat transfer between the solar absorber and the air in the cavity is much easier to be conducted because of the short distance and small mass of the air. It can also be noticed that the air velocity shows a little fluctuation for those experimental data obtained by Ryan [23]. The fluctuation may be because of the high air velocity as some of the low air velocity follows this rule quite well based on the same test rig.

Fig. 4(b) shows the influences of cavity gap on volumetric flow rate. A total opposite phenomenon can be seen that it increases with a bigger cavity gap even for a cavity gap of 0.6 m. This is because the mass of air in the cavity increases and more air is then heated up, resulting in relatively high airflow rate. However, the mass of the air should be within the heating capacity of the solar absorber, otherwise the flow may drop because of the reverse flow caused by unheated air. This obeys well with the results from Gan [36] that there existed an optimum cavity width for maximising the buoyancy-induced flow rate and the optimum width was between 0.55 and 0.6 m for a 6.0 m high solar chimney.

To determine the influence of air gap on the air velocity, it can be obtained following Ryan [32],

$$u_i = a_i \cdot d^{b_i} \tag{8}$$

Using the log on both sides of Eq. (8) gives,

$$log(u_i) = b_i \cdot log(d) + log(a_i) \tag{9}$$

Following Eq. (9), the b_i for experimental data from different test rigs can be obtained by regression. The b can be then calculated by,

$$b = \sum_{i=1}^{N} \frac{b_i}{N} \tag{10}$$

Based on Eqs. (8)–(10), the relationship between the air velocity and cavity gap from different test rigs can be obtained, shown in Fig. 5(a). For the regression, the R^2 values and slopes are shown in the upper left corner of Fig. 5(a), same applied to the following figures. The relationship can be expressed by,

$$u \propto d^{-0.44} \tag{11}$$

It is known that the volumetric flow rate can be calculated by the air velocity and cross-section area of the cavity. After combining this relationship with Eq. (11), the volumetric flow rate should be linear to $d^{0.56}$. However, it does not correlate very well. So we use an averaged exponents from the correlations obtained by Ryan et al. [24,26,32]. The volumetric flow rate correlates quite well under this situation, shown in Fig. 5(b). The relationship can be expressed by,

$$\overline{V} \propto d^{0.7} \tag{12}$$

4.3. Cavity height

The experimental studies on the influence of cavity height are very limited. From all the experimental tests collected in this study, only two tests were found by varying cavity heights. Fig. 6 shows the relationship between solar chimney performance and cavity height. Not surprisingly, both air velocity and volumetric flow rate

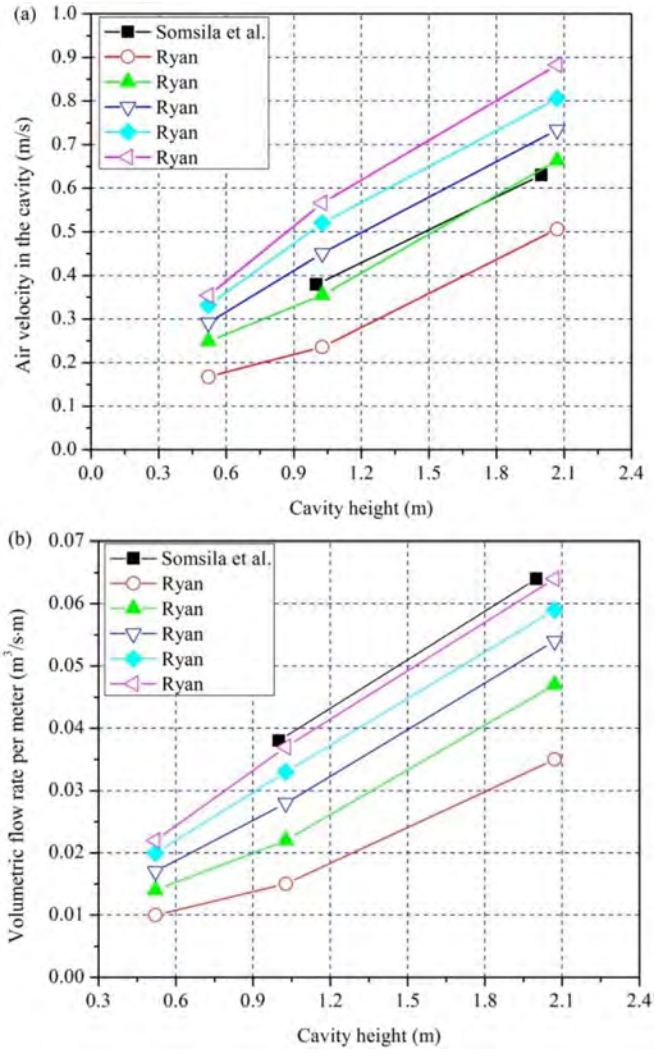

Fig. 6. The influence of cavity height on: (a) air velocity in the cavity; and (d) volumetric flow rate.

increase with a higher cavity height. This is due to the increasing area of solar absorber for heating up the air in the cavity. It is known that increasing the height of solar chimney can enhance the ventilation and also is profitable to obtain favourable pressure difference distribution [37]. Du et al. [38] suggested that the maximum mass flow rate can be achieved by choosing the longest vertical length within the restriction of the building code.

From previous mathematical models, listed in Table 3, it is obtained that the volumetric flow rate is linear respect to $H^{1/2}$, $H^{0.539}$, $H^{0.6}$ and $H^{2/3}$. The correlations between air velocity and cavity height are shown in Fig. 7. It is observed that the air velocity and $H^{2/3}$ shows the best fit among these four situations. It is expressed by,

$$u \propto H^{2/3} \tag{13}$$

Similarly, the experimental volumetric flow rate correlate the best with $H^{2/3}$, shown in Fig. 8. This is determined by the relationship between these volumetric flow rate and air velocity, where the volumetric flow rate is the product of averaged air velocity in the cavity and cross-section area. It can be given by,

$$\overline{V} \propto H^{2/3} \tag{14}$$

4.4. Height/cavity gap ratio

The relationship between solar chimney performance and height or cavity gap has been addressed in above sections. In the previous experimental studies, shown in Fig. 9, a range of 2.5–103.5 for height/cavity gap ratio was addressed. The trends for solar chimney performance and H/d are opposite to those of cavity gap. It is known from Fig. 9 that the air velocity increases with a larger H/d, and the indirect relationship between volumetric flow rate and H/d is in an opposite way. This may indicate that compared to cavity height, cavity gap plays a more important role in determining the cavity performance. For example, it is known that the volumetric flow rate increases when cavity height goes up. However, the increasing rate for a higher height is less than the decreasing rate by the decreasing cavity gap, resulting in a lower volumetric flow rate, shown in Fig. 9(b). Afonso and Oliveira [17] found a similar phenomenon that it is better to have a large chimney width and a smaller height.

It is noticed from Fig. 9 that the measured air velocity by Ryan [23] fluctuate increasingly with H/d, which is similar to that of cavity gap. Furthermore, some studies for low H/d show a different trend for other type of solar chimney, such as Trombe wall. Mathur et al. [39] analysed nine different combinations of H/d for a Trome wall and a maximum ventilation of was reported at an H/d of 2.83 for a 1 m high chimney with different absorber height ranging from 0.7 m to 0.9 m. A numerical study showed that there is an optimum ratio (10 in most cases) for Trombe wall to achieve a maximum airflow rate, which is dependent on the inlet design and independent of solar radiation [40].

4.5. Inlet and outlet areas

As mentioned above, only one experimental test by Susanti et al. [19] has been found in the literature regarding outlet/inlet ratio (A_{out}/A_{in}). In this test, the inlet and outlet openings were covered by

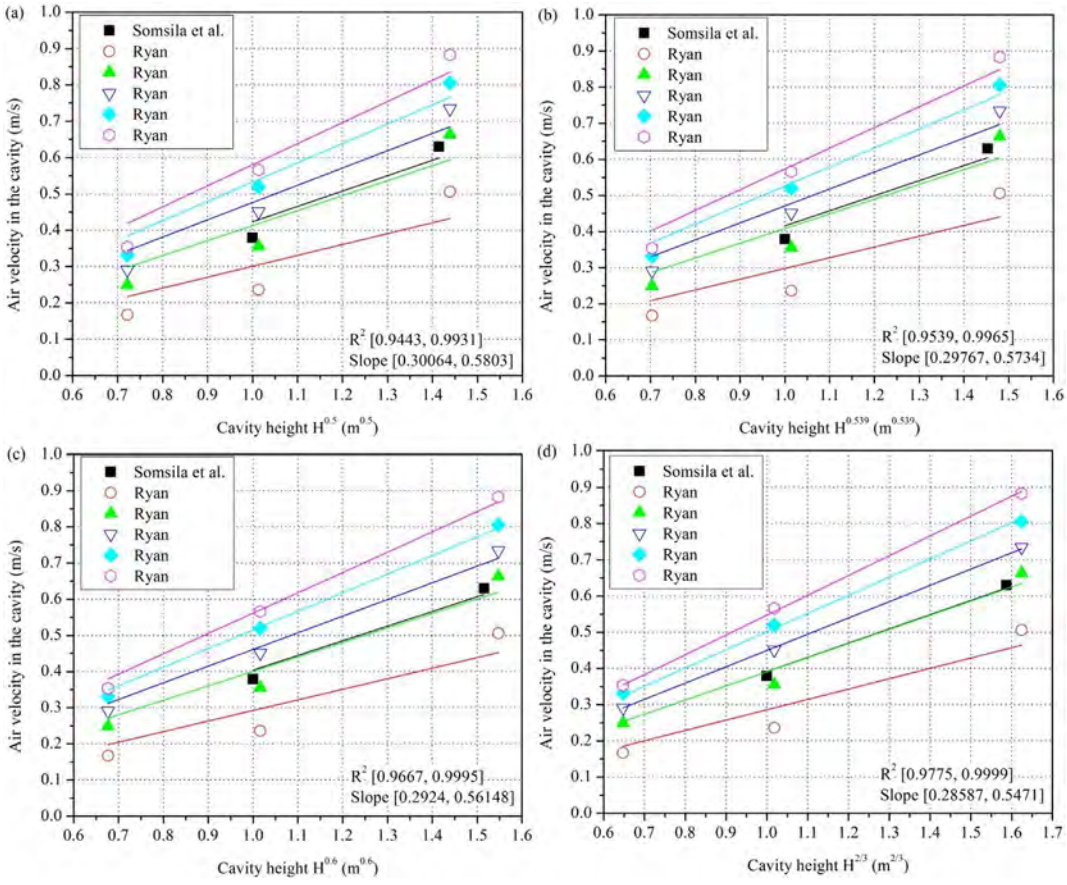

Fig. 7. Correlation between air velocity in the cavity and cavity height: (a) $H^{0.5}$; (b) $H^{0.539}$; (c) $H^{0.6}$; and (d) $H^{2/3}$.

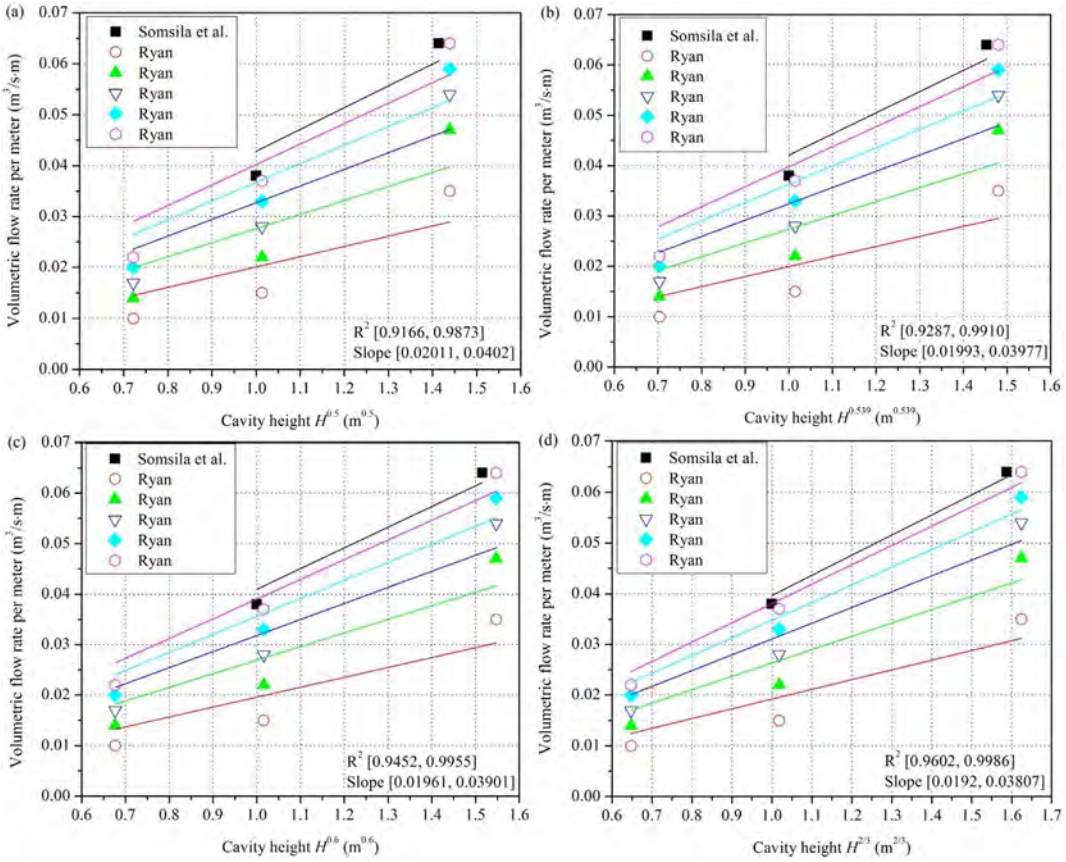

Fig. 8. Correlation between volumetric flow rate and cavity height: (a) $H^{0.5}$; (b) $H^{0.539}$; (c) $H^{0.6}$; and (d) $H^{2/3}$.

aluminium plates to construct various opening ratios, while the cross-section area of the cavity was kept the same. For the rest of tests of this study, the inlet, outlet and cross-section areas of the cavity are the same. So the influence of inlet and outlet areas on solar chimney performance for this kind of tests is the same with cavity gap.

For the only experimental test found in the literature regarding inlet and outlet areas, the influence of A_{out}/A_{in} on the volumetric flow rate can be seen in Fig. 10. The fractions in this figure represent the ratio of outlet and inlet area, and the numerator and denominator in these fractions are the outlet and inlet areas, respectively. It is known that the equal inlet and outlet area can enhance the airflow rate in the cavity. For example, among these six cases with unequal inlet and outlet, there are two cases shows a smaller airflow rate than equal cases even though they have much bigger inlet area, such as 4/312 and 8/312. This may be also proved by a numerical study [41] that optimized ventilation flow rate can be obtained when the outlet takes the same area as the inlet.

It can also be known from Fig. 10 that the outlet area show more importance in promoting the air flow for unequal openings. For example, the cases with 312/14, 312/8 and 312/4 show higher airflow than those with 14/312, 8/312 and 4/312 opening ratios. This trend is even obvious with a small inlet or outlet area. An analytical study by Bassiouny and Koura [42] shows similar phenomenon that three times of the inlet area can only improve the air change per hour (ACH) by almost 11%. This is probably because of the pressure loss through inlet and outlet. Comparing to inlet, the pressure loss through the outlet is relatively small. This can be reflected by the pressure loss coefficient that they are considered as 1.5 and 1.0, respectively, for inlet and outlet [16]. Under the situation, the increase of the outlet area is more efficient to improve the performance.

4.6. Radiation heat

It is quite clear that high radiation intensity can enhance the performance of solar chimney. It can be explained by buoyancy theory that a bigger temperature difference can result in a higher pressure difference, which is the driven force for air movement in the cavity. The same phenomenon can be seen in Fig. 11. Both air velocity and volumetric flow rate shows a bigger value with a higher radiation flux. Same phenomenon can be found in many previous studies. Bansal et al. [33] estimated that for a solar chimney with surface area of 2.25 m^2 the airflow rate can increase from 100 m^3/h to 350 m^3/h when solar radiation rises from 100 W/m^2 to 1000 W/m^2. A numerical study by Manca et al. [43] showed an increase of both velocity and mass flow rate after rising the heating flux of wall.

Based on the method expressed in Eqs. (8)–(10), the correlations between the solar chimney performance and radiation heat are conducted. The correlation between air velocity and radiation heat can be seen in Fig. 12(a). It can be observed from this figure that the measured air velocity from all the analysed test rigs correlate with radiation heat by,

$$u \propto q^{0.37} \tag{15}$$

Similarly, relationship between the volumetric flow rate and

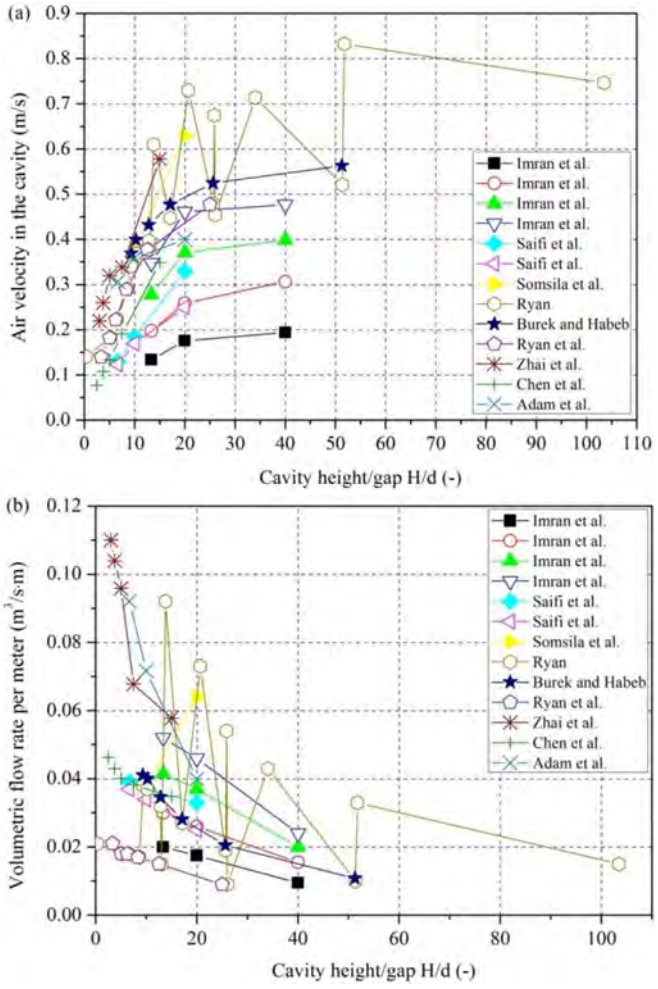

Fig. 9. The influences of cavity height/gap ratio on: (a) air velocity in the cavity; and (b) volumetric flow rate.

radiation heat can be obtained. The power exponent of 0.5 is a little higher than those obtained by Ryan [32,26]. The relationship obtained by all the experimental data collected from different test rigs can be expressed by,

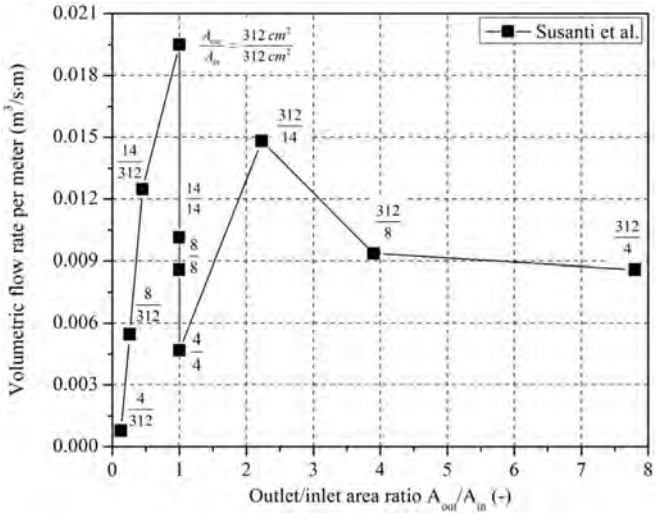

Fig. 10. The influence of outlet/inlet area ratio on volumetric flow rate per meter.

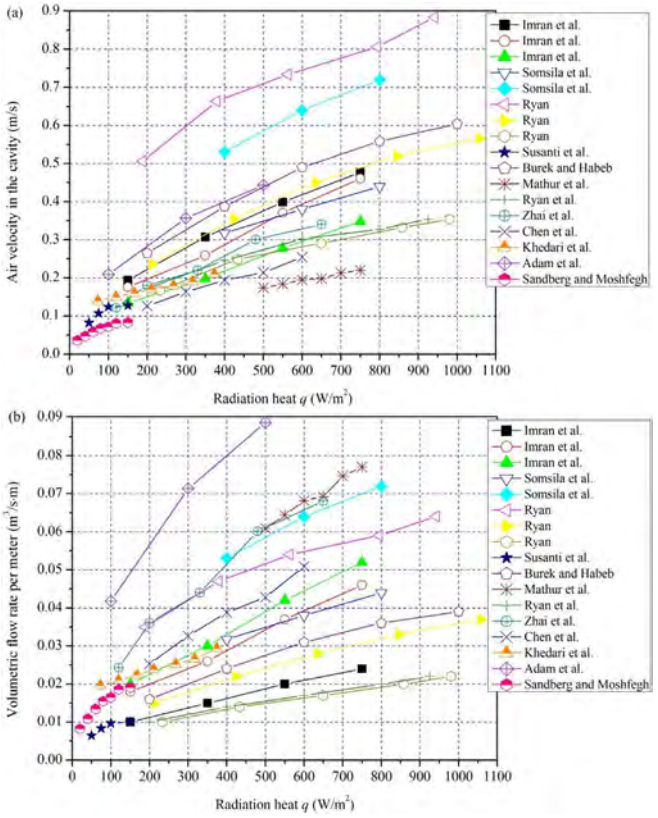

Fig. 11. The influence of radiation heat on: (a) air velocity in the cavity; and (b) volumetric flow rate per meter.

$$\overline{V} \propto q^{1/2} \tag{16}$$

5. Development of empirical model

In above sections, the influences of inclination angle, cavity gap, height, height/cavity gap ratio, inlet and outlet area, and radiation heat on the solar chimney performance have been addressed. It is known that the volumetric flow rate is linearly related to $(\sin\theta')^{1/3}$, $d^{0.7}$, $H^{2/3}$ and $q^{1/2}$. During these correlations, the volumetric flow rate per meter wide cavity was used. Therefore, a relationship is proposed to predict the volumetric flow rate under different conditions,

$$V = a \cdot w(sin\theta')^{1/3} q^{1/2} d^{0.7} H^{2/3} \tag{17}$$

Based on Eq. (17), the correlations between V and $w(\sin\theta')^{1/3}q^{1/2}d^{0.7}H^{2/3}$ are shown in Fig. 13. Those experimental data from Saifi et al. [21] and Susanti et al. [19] were not included in the correlation because no radiation heat was mentioned and restricted inlet and outlet were considered in the experiments, respectively. It is observed they correlate quite well with $w(\sin\theta')^{1/3}q^{1/2}d^{0.7}H^{2/3}$, showing a slope range between 76 and 176. A smaller slope refers to a bigger predicted volumetric flow rate. The maximum slope was observed for the experimental data by Imran et al. [20]. The related regression results can also be seen in Table 4. It is observed that the correlations are quite good, showing a high R^2 value range of 0.9435–0.9997.

To address the influencing factors on the slope obtained from

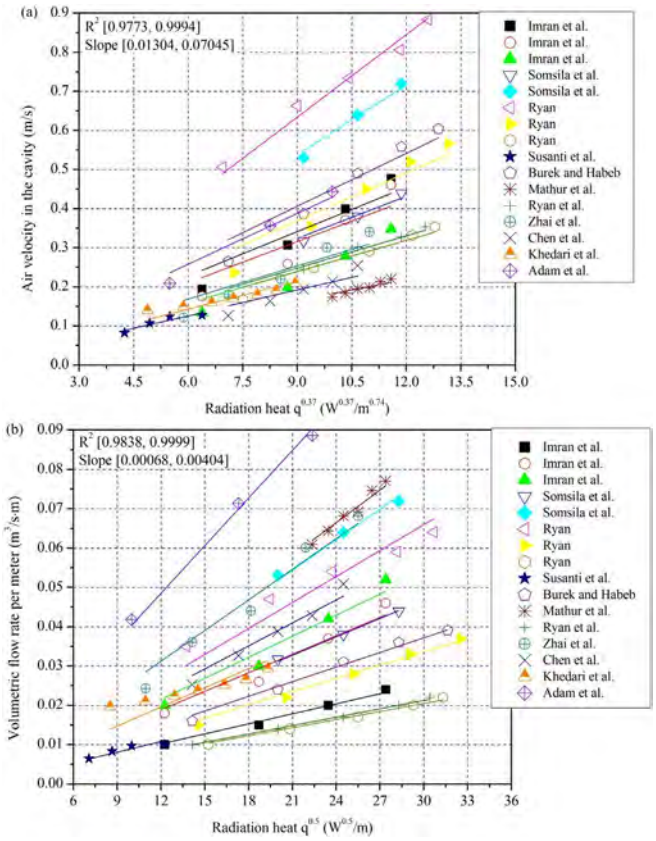

Fig. 12. Correlation between radiation heat and: (a) air velocity in the cavity; and (b) Volumetric flow rate per meter.

regression, a summary of the test conditions was provided in Table 4, including the latitude of test location, test environment, cavity material, glazing, heating and insulation. For the latitude, no trend can be observed from the collected experimental tests. This is probably because some of the tests were taken in stable indoor environment, and some others were performed in outdoor conditions which can be affected by many influencing factors. Two heating methods were found in previous tests, namely outdoor solar radiation and indoor self-heating. This is consistent with the test environment. Therefore, the latitude and heating method will not be considered in the following analysis.

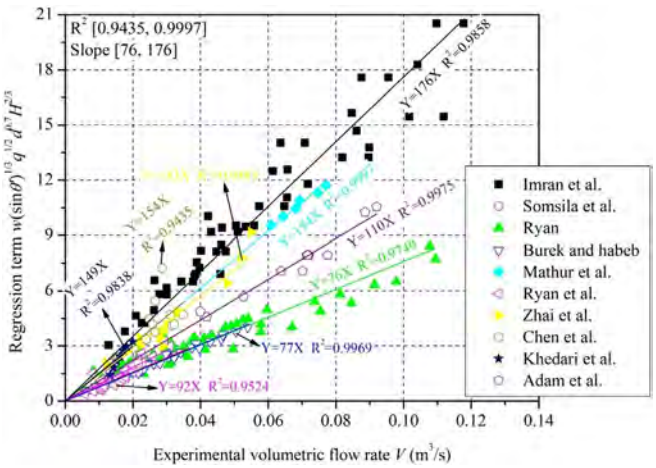

Fig. 13. Correlation between experimental volumetric flow rate and influencing factors.

The influencing factors on the slopes obtained from the regression between the experimental airflow rate V and $w(\sin\theta')^{1/3}q^{1/2}d^{0.7}H^{2/3}$ can be seen in Fig. 14. The column in this figure is the average slope and error bar shows the range of slopes under the situation listed in Table 4. The objective of this figure is to address the influences of some factors, such as test environment, cavity material, glazing, and insulation, on the performance of roof solar chimney. A smaller slope means an enhanced performance of solar chimney.

It can be seen from Fig. 14 that the experimental tests with outdoor environment, metal cavity, non-glazing and normal insulation show high slopes. For outdoor tests, the results are still affected by the external wind even those tests have taken measures to reduce the influence. The same phenomenon was observed by Tan and Wong [44] that external wind can improve the air speed in the solar chimney. All the metal structured cavities show high slopes. This is because comparing to wood and plasterboard, metal can accelerate the heat exchange with outside air under high thermal conductivity. Tests with glazing at the surface of chimney cavity and heavy insulation are showing low slopes, which are also beneficial to the improvement of the performance. It should be noticed that the heavy insulation means the thickness of insulation is around 5 cm or above in this study. This is following Afonso and Oliveira [17] that a thickness of 5 cm insulation wall is sufficient for solar chimney.

Based on the above analysis, it is known that these four factors have influences on the slope. Regression based on dichotomous variables is then used to determine the influence quantitatively. The tests with outdoor environment, metal structured cavity, non-glazing and normal insulation have the input of 1, otherwise it will be 0. The relationship can be given by,

$$Slope = 37E + 50M + 66G - 4I + 82 \quad (18)$$

where E is the environmental factors, while 1 for outdoor test and 0 for indoor test; M is the cavity materials, while 1 for metal structured cavity and 0 for others; G is the glazing, while 1 for non-glazing and 0 for glazing; and I is the insulation, while 0 for heavy insulation with a thickness near 5 cm or above and 1 for normal insulation.

Based on Eq. (18), the predicted slopes show an average error of 7.6% and the errors are within a range of −14.3% to 20%. From the coefficient of these four factors, it can be known that the glazing has the biggest influence on the slope, showing a coefficient of 66. The following factors are cavity materials, test environment and insulation, with a coefficient of 50, 37, and −4, respectively.

The comparison between experimental and predicted volumetric flow rate of solar chimney can be seen in Fig. 15. It is observed that these two correlate well, showing a good trend for the predictions. The average errors for the prediction of various test rigs are within a range of −16.2% and 16.1%. The two worst predictions are the predictions for the experimental results obtained from Chen et al. [28] and Adam et al. [30]. For the predictions of all the test rigs, the overall average error is 14%, and the errors are within a range of −30% to 144.6%.

The empirical model obtained based on experimental data from various test rigs can be obtained to predict the volumetric flow rate in the cavity of a roof solar chimney,

Table 4
A summary of potential factors on the slope obtained from regression.

Test rig	Regression	R^2	Latitude (°)	Test environment	Cavity material	Glazing	Heating	Insulation
Imran et al. [20]	Y = 176X	0.9858	33.3	Outdoor	Aluminium	Glass	Solar radiation	Regular[b]
Somsila et al. [22]	Y = 79X	0.9992	15.8[a]	Indoor	Wood	Glass	Artificial lighting	Regular[b]
Ryan [23]	Y = 76X	0.9749	55.8	Indoor	Plasterboard	Perspex	Electric heating mat	13 cm insulation
Burek and Habeb [24]	Y = 77X	0.9969	55.8	Indoor	Plasterboard	Perspex	Electric heating mat	10 cm insulation
Mathur et al. [25]	Y = 154X	0.9997	26.9	Outdoor	Aluminium	Glass	Solar radiation	2.5 cm thermocol sheet
Ryan et al. [26]	Y = 92X	0.9524	55.8	Indoor	Plasterboard	Perspex	Electric heating mat	10 cm rockwool
Zhai et al. [27]	Y = 143X	0.9888	31.2	Indoor	Wood	Wood	Electric heating plate	1 cm glass wool
Chen et al. [28]	Y = 154X	0.9435	37.8[a]	Indoor	Stainless-steel	Plexiglas	Self-heating plate	10 cm fiberglass
Khedari et al. [29]	Y = 149X	0.9838	15.8	Indoor	Plywood	Plywood	Plate heater	4.7 cm wool
Adam et al. [30]	Y = 110X	0.9975	34.7	Indoor	Aluminium	Glass	Electrically heated panel	Heavily insulated

Note.
[a] There is no specific description of experimental location in the context, so the locations of the first author were used; and
[b] It means regular insulation which was not specially indicated in the literatures.

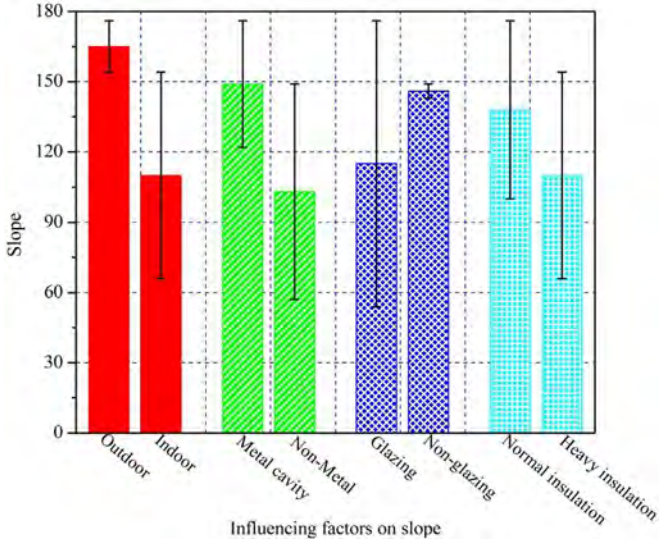

Fig. 14. The influencing factors on the slopes obtained from the regression between the experimental airflow rate V and $w(\sin\theta')^{1/3}q^{1/2}d^{0.7}H^{2/3}$; and a small slope means an enhanced performance of solar chimney.

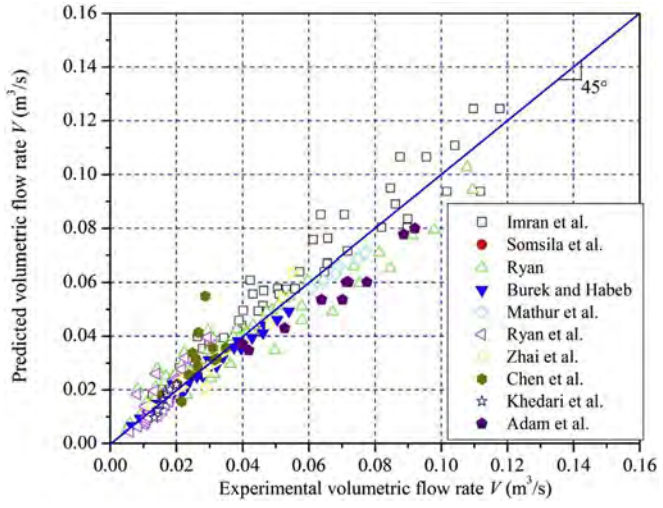

Fig. 15. A comparison between experimental and predicted volumetric flow rate by Eq. (19).

$$V = \frac{w(sin\theta')^{1/3}q^{1/2}d^{0.7}H^{2/3}}{Slope}, where\ \theta' = \begin{cases} \theta, & \theta \le 52.5 \\ 105-\theta, & \theta > 52.5 \end{cases}; Slope\ in\ Eq.(18) \quad (19)$$

One of the advantages of this empirical model is based on inputs which are easy to be obtained, such as cavity width, radiation heat, inclination angle, air gap thickness, and chimney height. As it is obtained by combining the experimental data from all the possible test rigs, this empirical model is then more generally applicable to different test configurations. The obtained empirical model can also largely improve the accuracy of prediction, which can be seen in Figs. 2 and 15, respectively.

6. Conclusions

To provide a reliable model to predict the performance of roof solar chimney, experimental data from all the possible test rigs are collected and analysed to address the influencing factors, such as inclination angle (θ), cavity gap (d), height (H), width (w), height/cavity gap ratio (H/d), inlet (A_{in}) and outlet area (A_{out}) and radiation heat (q). An empirical model is developed and validated by experimental data from various test rigs,

$$V = \frac{w(sin\theta')^{1/3}q^{1/2}d^{0.7}H^{2/3}}{Slope}, where\ \theta' = \begin{cases} \theta, & \theta \le 52.5 \\ 105-\theta, & \theta > 52.5 \end{cases}; Slope\ in\ Eq.(18)$$

In above empirical model, θ' is called calculated inclination angle from the horizontal. It shows good prediction for inclination angle during a range from 10° to 90°. The slope in the empirical model can be determined by Eq. (18) through four influencing factors, including test environment, cavity material, glazing, and insulation. It is known that the glazing conditions show the highest influence to the slope, following by cavity material, test environment, and insulation conditions. The prediction of the empirical model shows an average error of 14% with the experimental results from various test rigs.

For the influencing factors, experimental data from various test rigs show that the volumetric flow rate decreases under a larger height-to-gap ratio within 2.5–103.5, and the air velocity is in an opposite way. For the inlet and outlet areas, it is indicated that an equal inlet and outlet area can enhance the airflow rate of the solar chimney, and outlet area shows a relatively higher importance to the performance of solar chimney.

It is not surprising that the available experimental tests are very limited in the literature, especially for cavity height (within a range of 0.521–2.07 m) and outlet/inlet area ratio (a range of 0.128–7.8), and more experimental tests are critically needed. For future tests, it is suggested to include all the possible information to benefit the relevant research, such as test location, detailed configuration of cavity and room, measurement techniques, and materials used for cavity.

References

[1] H.H. Al-Kayiem, K.V. Sreejaya, S.I.U. Gilani, Mathematical analysis of the influence of the chimney height and collector area on the performance of a roof top solar chimney, Energy Build. 68 (2014) 305–311.

[2] D.S. Lee, T.C. Hung, J.R. Lin, J. Zhao, Experimental investigations on solar chimney for optimal heat collection to be utilized in organic Rankine cycle, Appl. Energy 154 (2015) 651–662.

[3] L. Shi, M.Y.L. Chew, A review on sustainable design of renewable energy systems, Renew. Sustain. Energy Rev. 16 (2012) 192–207.

[4] H.R. Li, Y.B. Yu, F.X. Niu, M. Shafik, B. Chen, Performance of a coupled cooling system with earth-to-air heat exchanger and solar chimney, Renew. Energy 62 (2014) 468–477.

[5] R. Khanal, C.W. Lei, Solar chimney - a passive strategy for natural ventilation, Energy Build. 43 (2011) 1811–1819.

[6] S. Lal, S.C. Kaushik, P.K. Bhargav, Solar chimney: a sustainable approach for ventilation and building space conditioning, Int. J. Dev. Sustain. 2 (2013) 1–21.

[7] G.H. Gan, A parametric study of Trombe walls for passive cooling of buildings, Energy Build. 27 (1998) 37–43.

[8] J. Khedari, N. Rachapradit, J. Hirunlabh, Field study of performance of solar chimney with air-conditioned building, Energy 28 (2003) 1099–1114.

[9] T. Miyazaki, A. Akisawa, T. Kashiwagi, The effects of solar chimneys on thermal load mitigation of office buildings under the Japanese climate, Renew. Energy 31 (2006) 987–1010.

[10] Q.Y. Chen, Ventilation performance prediction for buildings: a method overview and recent applications, Build. Environ. 44 (2009) 848–858.

[11] D. Fidaros, C. Baxevanou, Numerical study of the natural ventilation in a dwelling with a solar chimney, in: The 3rd International Conference on Passive & Low Energy Cooling for the Built Environment, Rhodes Island, Greeze, 2010.

[12] B. Zamora, A.S. Kaiser, Optimum wall-to-wall spacing in solar chimney shaped channels in natural convection by numerical investigation, Appl. Therm. Eng. 29 (2009) 762–769.

[13] R. Khanal, C.W. Lei, Numerical investigation of the ventilation performance of a solar chimney, ANZIAM J. 52 (2011) 899–913.

[14] L. Shi, G.M. Zhang, An empirical model to predict the performance of typical solar chimneys considering both room and cavity configurations, Build. Environ. 103 (2016) 250–261.

[15] E.P. Sakonidou, T.D. Karapantsios, A.I. Balouktsis, D. Chassapis, Modeling of the optimum tilt of a solar chimney for maximum air flow, Sol. Energy 82 (2008) 80–94.

[16] J. Halldorsson, C. Byrjalsen, Z.D. Chen, P. Bandopadhayay, P. Heiselberg, Experimental and theoretical studies of a solar chimney with uniform heat flux, in: The 8th International Conference on Air Distribution in Rooms, Copenhagen, Denmark, 2002, pp. 597–600.

[17] C. Afonso, A. Oliveira, Solar chimneys: simulation and experiment, Energy Build. 32 (2000) 71–79.

[18] M. Sandberg, B. Moshfegh, Ventilated-solar roof air flow and heat transfer investigation, Renew. Energy 15 (1998) 287–292.

[19] L. Susanti, H. Homma, H. Matsumoto, Y. Suzuki, M. Shimizu, A laboratory experiment on natural ventilation through a roof cavity for reduction of solar heat gain, Energy Build. 40 (2008) 2196–2206.

[20] A.A. Imran, J.M. Jalil, S.T. Ahmed, Induced flow for ventilation and cooling by a solar chimney, Renew. Energy 78 (2015) 236–244.

[21] N. Saifi, N. Settou, B. Dokkar, B. Negrou, N. Chennouf, Experimental study and simulation of airflow in solar chimneys, Energy Procedia 18 (2012) 1289–1298.

[22] P. Somsila, U. Teeboonma, W. Seehanam, Investigation of buoyancy air flow inside solar chimney using CFD technique, in: The International Conference on Energy and Sustainable Development: Issues and Strategies, Chiang Mai, Thailand, 2010, pp. 1–7.

[23] D. Ryan, Experimental Investigation of Buoyancy Driven Natural Convection for Solar Applications in Building Facades, PhD thesis, Glasgow Caledonian University, 2008.

[24] S.A.M. Burek, A. Habeb, Air flow and thermal efficiency characteristics in solar chimneys and Trombe Walls, Energy Build. 39 (2007) 128–135.

[25] J. Mathur, S. Mathur, Anupma, Summer-performance of inclined roof solar chimney for natural ventilation, Energy Build. 38 (2006) 1156–1163.

[26] D.A. Ryan, S. Burek, P. Baker, Experimental investigation into the buoyancy driven convection in passive solar heating facades, in: The 2nd Scottish Conference for Postgraduate Researchers of the Built and Natural Environment, Glasgow Caledonian University, UK, 2005, pp. 683–693.

[27] X.Q. Zhai, Y.J. Dai, R.Z. Wang, Experimental investigation on air heating and natural ventilation of a solar air collector, Energy Build. 37 (2005) 373–381.

[28] Z.D. Chen, P. Bandopadhayay, J. Halldorsson, C. Byrjalsen, P. Heiselberg, Y. Li, An experimental investigation of a solar chimney model with uniform wall heat flux, Build. Environ. 38 (2003) 893–906.

[29] J. Khedari, P. Yimsamerjit, J. Hirunlabh, Experimental investigation of free convection in roof solar collector, Build. Environ. 37 (2002) 455–459.

[30] Z. Adam, T. Yamanaka, H. Kotani, Mathematical model and experimental study of airflow in solar chimneys, in: The 8th International Conference on Air Distribution in Rooms, Technical University of Denmark, Denmark, 2002, pp. 621–624.

[31] S.J. Emmerich, W. Stuart Dols, J.W. Axley, Natural Ventilation Review and Plan for Design and Analysis Tools Report, Report No.: NISTIR 6781, National Institute of Standards and Technology, 2001.

[32] D. Ryan, S.A.M. Burek, Experimental study of the influence of collector height on the steady state performance of a passive solar air heater, Sol. Energy 84 (2010) 1676–1684.

[33] N.K. Bansal, R. Mathur, M.S. Bhandari, Solar chimney for enhanced stack ventilation, Build. Environ. 28 (1993) 373–377.

[34] H.B. Awbi, G. Gan, Simulation of solar-induced ventilation, in: The 2nd World Renewable Energy Congress, Reading, UK, 1992, pp. 2016–2030.

[35] C.J. Hocevar, R.L. Casperson, Thermocirculation data and instantaneous efficiencies for Trombe walls, in: The 4th National Passive Solar Conference, Kansas, USA, 1979, pp. 163–167.

[36] G.H. Gan, Simulation of buoyancy-induced flow in open cavities for natural ventilation, Energy Build. 38 (2006) 410–420.

[37] W.T. Ding, Y. Hasemi, T. Yamada, Natural ventilation performance of a double-skin façade with a solar chimney, Energy Build. 37 (2005) 411–418.

[38] W. Du, Q.R. Yang, J.C. Zhang, A study of the ventilation performance of a series of connected solar chimneys integrated with building, Renew. Energy 36 (2011) 265–271.

[39] J. Mathur, N.K. Bansal, S. Mathur, M. Jain, Anupma, Experimental investigations on solar chimney for room ventilation, Sol. Energy 80 (2006) 927–935.

[40] L.P. Wang, A.G. Li, A numerical study of Trombe wall for enhancing stack ventilation in buildings, in: The 23rd Conference on Passive and Low Energy Architecture, Geneva, Switzerland, 2006.

[41] A.G. Li, P. Jones, P.G. Zhao, L.P. Wang, Heat transfer and natural ventilation airflow rates from single-sided heated solar chimney for buildings, J. Asian Archit. Build. Eng. 3 (2004) 233–238.

[42] R. Bassiouny, N.S.A. Koura, An analytical and numerical study of solar chimney use for room natural ventilation, Energy Build. 40 (2008) 865–873.

[43] O. Manca, S. Nardini, P. Romano, E. Mihailov, Numerical investigation of thermal and fluid dynamic behavior of solar chimney building systems, J. Chem. Technol. Metallurgy 49 (2014) 106–116.

[44] A.Y.K. Tan, N.H. Wong, Influences of ambient air speed and internal heat load on the performance of solar chimney in the tropics, Sol. Energy 102 (2014) 116–125.